

## Neutron halo in $^{14}\text{B}$ studied via reaction cross sections

M. Fukuda<sup>1,a</sup>, D. Nishimura<sup>2</sup>, S. Suzuki<sup>3</sup>, M. Tanaka<sup>1</sup>, M. Takechi<sup>4</sup>, K. Iwamoto<sup>1</sup>, S. Wakabayashi<sup>1</sup>, M. Yaguchi<sup>1</sup>, J. Ohno<sup>1</sup>, Y. Morita<sup>1</sup>, Y. Kamisho<sup>1</sup>, M. Mihara<sup>1</sup>, K. Matsuta<sup>1</sup>, M. Nagashima<sup>3</sup>, T. Ohtsubo<sup>3</sup>, T. Izumikawa<sup>5</sup>, T. Ogura<sup>3</sup>, K. Abe<sup>3</sup>, N. Kikukawa<sup>3</sup>, T. Sakai<sup>3</sup>, D. Sera<sup>3</sup>, T. Suzuki<sup>6</sup>, T. Yamaguchi<sup>6</sup>, K. Sato<sup>6</sup>, H. Furuki<sup>6</sup>, S. Miyazawa<sup>6</sup>, N. Ichihashi<sup>6</sup>, J. Kohno<sup>6</sup>, S. Yamaki<sup>6</sup>, A. Kitagawa<sup>7</sup>, S. Sato<sup>7</sup>, and S. Fukuda<sup>7</sup>

<sup>1</sup>Department of Physics, Osaka University, Toyonaka, Osaka 560-0043, Japan

<sup>2</sup>Department of Physics, Tokyo University of Science, Noda 278-8510, Japan

<sup>3</sup>Department of Physics, Niigata University, Niigata 950-2102, Japan

<sup>4</sup>Gesellschaft für Schwerionenforschung GSI, 64291 Darmstadt, Germany

<sup>5</sup>RI center, Niigata University, Niigata 951-8510, Japan

<sup>6</sup>Department of Physics, Saitama University, Saitama 338-3570, Japan

<sup>7</sup>National Institute of Radiological Sciences, Chiba 263-8555, Japan

**Abstract.** Reaction cross sections ( $\sigma_R$ ) for the neutron-rich nucleus  $^{14}\text{B}$  on Be, C, and Al targets have been measured at several energies in the intermediate energy range of 45–120 MeV/nucleon. The present experimental  $\sigma_R$  show a significant enhancement relative to the systematics of stable nuclei. The nucleon density distribution was deduced through the fitting procedure with the modified Glauber calculation. The necessity of a long tail in the density distribution was found, which is consistent with the valence neutron in  $2s_{1/2}$  orbital with the small empirical one-neutron separation energy in  $^{14}\text{B}$ .

### 1 Introduction

For the formation of a neutron halo, a small one- or two-neutron separation energy and a small orbital angular momentum ( $\ell = 0$  or 1) are considered to be essential. In addition to these conditions, the actual neutron halo nuclei in the light mass region often show complex relation between the formation of halo and the level inversion or the existence of intruder levels. In order to understand such relations between energy shifts of levels, orbital angular momentum, and separation energy, finding and studying a lot of examples of neutron halo nuclei should be important.

For the neutron-rich nucleus  $^{14}\text{B}$ , the pioneering work of the nuclear size was the measurement of interaction cross sections by Tanihata et al. [1]. However, no significant indication of a neutron halo in  $^{14}\text{B}$  was observed in that work. After that, the electromagnetic moments of  $^{14}\text{B}$  were measured by Okuno et al. [2] and Izumi et al. [3] to point out the importance of  $2s_{1/2}$  orbital. On the other hand, the momentum distribution of  $^{13}\text{B}$  fragment produced in the projectile fragmentation of  $^{14}\text{B}$  beam was studied experimentally by Bazin et al. [4] and Guimarães et al. [5]. They found considerably small width of the momentum distribution that strongly supports the significant contribution of the  $2s_{1/2}$  component in the valence neutron configuration.

---

<sup>a</sup>e-mail: mfukuda@phys.sci.osaka-u.ac.jp

In the present work, we have measured reaction cross sections ( $\sigma_R$ ) for  $^{14}\text{B}$  at intermediate energies where  $\sigma_R$  is more sensitive to dilute densities like a halo compared to higher energies. From the energy dependence of  $\sigma_R$ , the nucleon density distribution of  $^{14}\text{B}$  has been deduced through the fitting procedure with the modified Glauber calculation. The experiment, analysis and preliminary results will be described as follows.

## 2 Experiment

The experiment was carried out at the HIMAC heavy ion synchrotron facility at National Institute for Radiological Sciences (NIRS), Japan. Primary beams of 160 MeV/nucleon  $^{18}\text{O}$  and 160 MeV/nucleon  $^{15}\text{N}$  were provided from the HIMAC synchrotron. In order to produce  $^{14}\text{B}$  secondary beams, the  $^{18}\text{O}$  beam impinged onto Be target and the  $^{15}\text{N}$  beam onto  $\text{CH}_2$  (polyethylene) target. The fragment separator beam line (SB2) [6] was used to separate  $^{14}\text{B}$  nuclei from others and to tune the beam energy. The  $^{14}\text{B}$  beams with intensities of 50–100 counts/spill and energies of 30–130 MeV/nucleon were focused onto the reaction target placed at the final focus (F3). The transmission method was employed to measure reaction cross sections. A schematic drawing of the experimental setup is shown in Fig. 1.

The particle identification (PID) upstream of the reaction target was performed by the  $B\rho$ -TOF- $\Delta E$  method. The time-of-flight (TOF) was measured between the first focus (F1) and F3 by using thin plastic counters. The energy loss ( $\Delta E$ ) was measured with the plastic counter at F3 that was also used for the stop counter for TOF measurement. The PID downstream of the reaction target was carried out by a  $\Delta E$ - $E$  counter telescope consisting of Si  $\Delta E$  counters and an NaI(Tl)  $E$  counter. For the measurements at higher incident energy of 130 MeV/nucleon, a thin CsI(Tl) counter was also used as a  $\Delta E$  counter in addition to Si counters.

Be, C, and Al plates, for which  $^{14}\text{B}$  has the same energy loss, were used as reaction targets. In order to correct for the amount of reactions at places other than the reaction target, e.g. inside the counters, the empty-target measurement was also performed. For the empty-target measurement, the incident beam energy at the entrance of downstream counters was tuned to be the same as that of target-in measurement by changing the combination of thicknesses of production target and wedge degrader. The  $\sigma_R$  is derived from  $\sigma_R = -\frac{1}{t} \ln\left(\frac{\Gamma}{\Gamma_0}\right)$ , where  $\Gamma$  is the ratio of the number of non-interacting outgoing nuclei to the number of incoming nuclei,  $\Gamma_0$  is the same ratio for the empty-target measurement, and  $t$  denotes the thickness of reaction target.

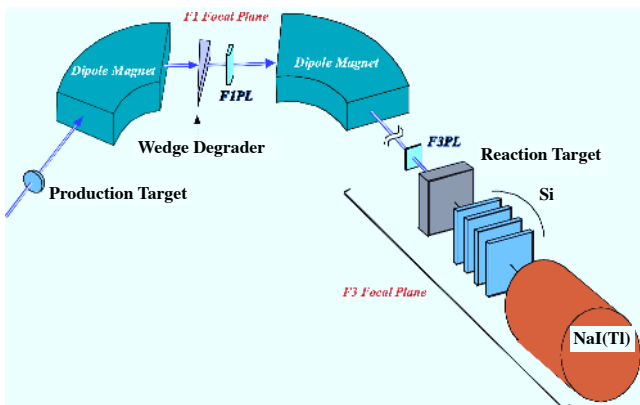


**Figure 1.** Schematic drawing of the experimental setup for the lower incident energy at 80 MeV/nucleon. At higher incident energy 130 MeV/nucleon, a thin CsI(Tl)  $\Delta E$  counter placed between Si and NaI(Tl) counters was also used.

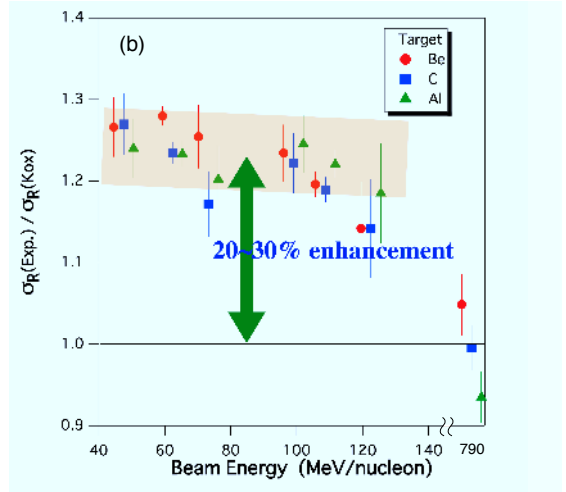
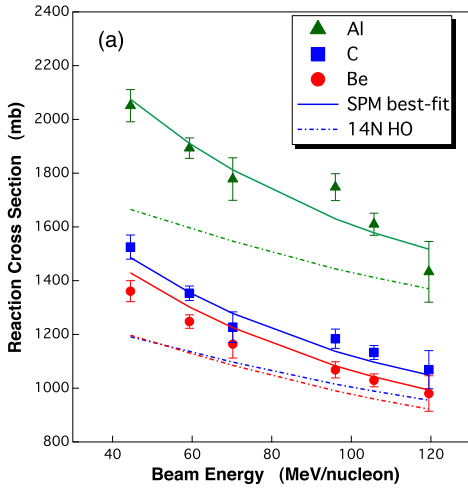


**Figure 2.** (a) Present experimental  $\sigma_R$  are indicated by solid symbols with error bars. Dash-dotted curves shows calculation with HO-type density for  $^{14}\text{B}$  using electron scattering parameters of  $^{14}\text{N}$ . The solid curves are the best-fit result of the fitting with the single-particle density for the valence neutron. (b) The ratio of  $\sigma_R$  data to the systematics by Kox et al. [7].

### 3 Results and Discussions

The present experimental  $\sigma_R$  are plotted by solid symbols as a function of beam energy in Fig. 2 (a). Figure 2 (b) shows the ratio of the experimental  $\sigma_R$  to the systematics of stable nuclei calculated with semi-empirical formula by Kox et al. [7]. As shown in Fig. 2 (b), the present data are enhanced by 20–30 % compared to the systematics of stable nuclei.

For more quantitative analyses, we utilized the modified Glauber calculation to connect the nucleon density distributions with the present  $\sigma_R$  data. This calculation can reproduce the experimental

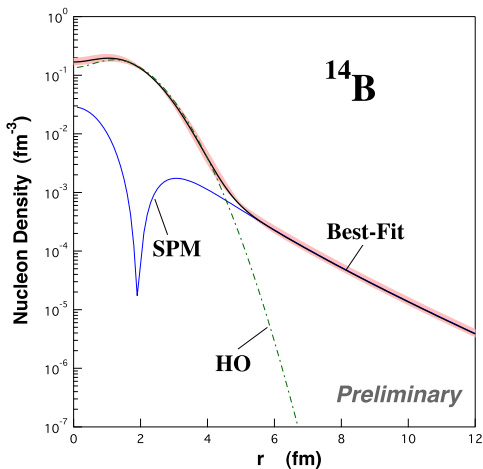


**Figure 3.** The preliminary result of best-fit nucleon density distribution for  $^{14}\text{B}$  assuming the single-particle model for the valence neutron is shown by the thick solid curve. The gray region indicates the error. HO-type distribution with the  $^{14}\text{N}$  electron-scattering parameters which corresponds to the calculated results (dash-dotted curves) in Fig. 2 (a) is also plotted by the dash-dotted curve. The single-particle density for the valence neutron (SPM) is shown by the thin solid curve.

$\sigma_R$  at intermediate and high energies quite well for both stable and unstable nuclei using their nucleon densities [8]. We first calculated  $\sigma_R$  using the harmonic-oscillator (HO) type density with  $^{14}\text{N}$  parameters determined by the electron scattering, which is shown by the dash-dotted curve in Fig. 3. This can not reproduce the data at all as shown by dash-dotted curves in Fig. 2 (a).

In order to deduce the nucleon density distribution of  $^{14}\text{B}$ , a fitting procedure was employed using the modified Glauber calculation assuming a model density [9, 10]. As a model function for the nucleon density distribution of  $^{14}\text{B}$ , the  $2s_{1/2}$ -orbital single-particle model (SPM) density for the valence neutron plus HO-type core was assumed with the experimental one-neutron separation energy of 0.97 MeV. The free parameters in the fitting were the core radius and the amplitude of the SPM density. The total integration of the density was normalized to 5 protons plus 9 neutrons. The preliminary result of the fitting is shown by the best-fit curve in Fig. 3 (thick solid curve). The gray region indicates the error of density. The HO-type density with the  $^{14}\text{N}$  parameters is also shown for comparison. From this comparison, it can be concluded that the tail component in the density distribution is necessary to reproduce the present  $\sigma_R$  data, especially at the lower energy part. This result shows that the present data is consistent with the model of the core plus one-neutron in s-orbital with the experimental separation energy for  $^{14}\text{B}$ . Detailed analyses are now in progress and will be reported elsewhere.

## Acknowledgements

The experiment in the present work was performed at NIRS-HIMAC under the research project with heavy ions. The authors are grateful to the staffs of HIMAC.

## References

- [1] I. Tanihata et al., Phys. Lett. **B206**, 592 (1988).
- [2] H. Okuno et al., Phys. Lett. **B354**, 41 (1995).
- [3] H. Izumi et al., Phys. Lett. **B366**, 51 (1996).
- [4] D. Bazin et al., Phys. Rev. **C57**, 2156 (1998).
- [5] V. Guimarães et al., Phys. Rev. **C61**, 064609 (2000).
- [6] M. Kanazawa et al., Nucl. Phys. A 746, 393c (2004).
- [7] S. Kox et al., Phys. Rev. **C35**, 1678 (1987).
- [8] M. Takechi et al., Phys. Rev. **C79**, 061601(R) (2009).
- [9] M. Fukuda et al., Phys. Lett. **B268**, 339 (1991).
- [10] K. Tanaka et al., Phys. Rev. **C82**, 044309 (2010).